Formation of $Al_2(MoO_4)_3$ and MoO_3 Phases Induced by Phosphate in Molybdena–Phosphorus Catalysts

R. LÓPEZ CORDERO,* S. LÓPEZ GUERRA,* J. L. G. FIERRO,†
AND A. LÓPEZ AGUDO†

*Centro de Investigaciones Químicas, Washington 169, La Habana, Cuba; and
†Instituto de Catálisis y Petroleoquímica, CSIC, Serrano 119, 28006-Madrid, Spain

The combined use of temperature-programmed reduction (TPR), Laser–Raman spectroscopy, and X-ray diffraction has provided evidence that phosphoric acid impregnation on γ-alumina, prior to molybdate incorporation, induces the formation of crystalline $Al_2(MoO_4)_3$ and MoO_3 species. These species, absent in the phosphorus-free preparations, are responsible for the appearance of an additional TPR peak at ca. 785 K and also for the development of characteristic Raman bands. © 1990 Academic Press, Inc.

INTRODUCTION

Phosphate as an additive to molybdenum-containing catalysts has been revealed as an intriguing component for hydroprocessing reactions (1–6). In order to understand the variety of functions ascribed to phosphate, some interesting studies have been performed in recent years (5–17). Most studies have established that (i) phosphate does not interact with the Mo phase, and (ii) it does not seem to be directly involved in the promotion action. The effect of phosphate on the hydrodesulfurization activity of Ni–Mo/Al_2O_3 catalysts has been ascribed to different distributions of Mo in the catalyst, which might favor the formation of the oxide precursor of the Ni–Mo–S phase (5, 10, 12), and to a better dispersion of the active components (10, 14).

Compared with molybdate, phosphate ions are preferentially adsorbed on alumina surfaces (7). As phosphate interacts very strongly with alumina, forming a surface $AlPO_4$ (13, 15, 18) upon calcination, it seems reasonable to assume that the presence of phosphate does not enhance the dispersion of molybdate in terms of the monolayer form, at least for catalysts prepared by se-

quential impregnation. Our own recent studies on Mo–P/Al_2O_3 catalysts revealed that the presence of phosphorus led to the formation of poorly dispersed molybdate species. The results of temperature-programmed reduction (TPR) and diffuse reflectance spectroscopy (DRS) on oxidic Mo–P/Al_2O_3 catalysts indicated clearly that phosphate addition increased the Mo fraction in easily reducible forms, such as multilayered molybdate species and probably formation of bulk MoO_3 at high P contents (16). In addition, X-ray photoelectron spectroscopy (XPS) and IR of adsorbed NO of the same sulfided catalysts revealed that phosphate leads to a Mo enrichment of the outer surface of the catalyst particles and favored the formation of larger MoS_2 structures (17). These effects were found to occur to a larger extent in the two-step prepared catalysts, in which phosphate was first impregnated, although they were also observed in coimpregnated samples.

In addition, high-resolution transmission electron microscopy of sulfided P-containing alumina-supported NiMo and CoMo catalysts has recently shown that when phosphate is present in the impregnation solution, the number of MoS_2 stacks in-

creases while the length of the MoS_2 crystallites decreases (12). These results also indicated that phosphate induces a lesser Mo dispersion, probably by formation of bulk MoO_3 in the oxidic state of phosphorus–molybdenum–alumina catalysts, at least when the former component is added as phosphate during the impregnation step.

In order to elucidate this particular effect of phosphate on the simpler catalytic system of unpromoted molybdenum catalysts, this work aims at the characterization by X-ray diffraction (XRD), Laser–Raman spectroscopy (LRS), and TPR techniques of some P-containing MoO_3/Al_2O_3 catalysts.

EXPERIMENTAL

Phosphorus-containing molybdena catalysts were prepared by two-step impregnation of γ-Al_2O_3 (Girdler T-126; surface area 190 m^2 g^{-1}; pore volume 0.39 cm^3 g^{-1}) with aqueous solutions of appropriate concentrations of orthophosphoric acid (Analar, reagent grade) in the first impregnation and ammonium heptamolybdate (BDH reagent grade) in the second. In all the impregnations the pH was adjusted to 1.5 (ca. the value corresponding to the maximum concentration of phosphoric acid used) by addition of dilute HNO_3 (BDH reagent grade). The excess water was removed in a rotary evaporator at 333 K and ca. 40 Torr. After each impregnation samples were dried at 393 K for 8 h and then calcined at 823 K for 4.5 h. The catalysts are hereafter referred to as Mo(x)–P(y), where x and y denote the weight percentages of MoO_3 and P_2O_5, respectively. An additional catalyst sample was obtained from the Mo(14)–P(4) one by leaching it with a 0.02% (v/v) ammonia solution for 15 min, followed by drying and calcination as above. This sample is hereafter referred to as Mo(14)–P(4)E.

XRD patterns were obtained with a Philips PW 1730/10 diffractometer operated at 40 kV and 33 mA with Ni-filtered $CuK\alpha$ radiation. Laser Raman spectra were recorded with a Jarrell–Ash spectrometer. The emission line at 514.5 nm from an Ar^+ laser was used for excitation. The sensitivity was adjusted according to the intensity of the Raman scattering.

TPR profiles were obtained using a thermoconductivity detector. Catalyst samples (0.25 g) were pretreated by heating linearly (10 K min^{-1}) from room temperature (rt) up to 833 K under an air flow (20 cm^3 min^{-1}). After 2 h at this temperature, the samples were allowed to cool to rt, and TPR experiments were performed by heating samples at a linear rate of 10 K min^{-1} from rt up to 1273 K. The reduction gas was a purified H_2/Ar mixture (molar ratio 7/3), and the flow rate 25 cm^3 min^{-1}.

The sample (Mo(14)–P(4) was also studied by XRD at different stages of reduction according to its TPR profile in a Parr high-temperature camera attached to the same diffractometer as described above. In this case, the experimental conditions and procedure were the same as those used in the TPR measurements. Reduction was stopped at selected points by flushing the camera with Ar and cooling the sample holder to rt.

RESULTS AND DISCUSSION

Figure 1 shows the XRD patterns of the four catalysts. The pattern of P-free Mo(14)–P(0) sample (Fig. 1a) shows only incipient peaks which could be ascribed to $Al_2(MoO_4)_3$. The XRD pattern of the Mo(14)–P(4) sample (Fig. 1b) shows diffraction lines of $Al_2(MoO_4)_3$ (ASTM 23-764) and of MoO_3 (ASTM 5-0508), indicating that the phosphate addition caused formation of bulk MoO_3 and $Al_2(MoO_4)_3$ crystallites of sizes above ca. 4 nm. The presence of both crystalline phases was also clearly observed for the Mo(8)–P(4) catalyst (Fig. 1c), which contains much less Mo loading and the same phosphorus content. At this point it must be noted that the P-free Mo(8)–P(0) counterpart gave a diffraction pattern similar to that of the alumina support, suggesting the absence of three-dimensional Mo-containing crystalline phases of crystal sizes above 4 nm. The Mo(14)–P(4)E catalyst (Fig. 1b') showed a similar behavior as no diffraction
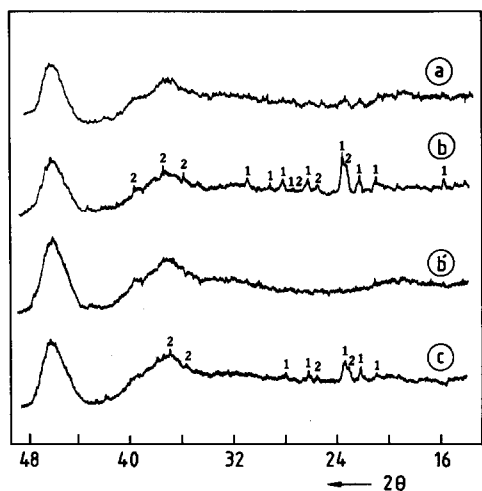
FIG. 1. X-ray diffraction patterns of catalysts: (a) Mo(14)–P(0), (b) Mo(14)–P(4), (b') Mo(14)–P(4)E, and (c) Mo(8)–P(4). Lines corresponding to (1) $Al_2(MoO_4)_3$ and (2) MoO_3.

peaks different from those of alumina were detected. In this case, both crystalline MoO_3 and $Al_2(MoO_4)_3$ weakly anchored on the alumina surface present on the Mo(14)–P(4) catalyst were removed by leaching with very dilute ammonia solution.

Additional evidence for the presence of bulk MoO_3 and $Al_2(MoO_4)_3$ was found by LRS. The spectra corresponding to the catalysts Mo(14)–P(0) and Mo(14)–P(4) and a reference MoO_3 compound are shown in Fig. 2. The spectrum of the sample Mo(14)–P(0) (Fig. 2a) showed two weak bands at 950 cm^{-1}, associated with molybdena–alumina interaction species (19–21 and references therein), and at 820 cm^{-1}, which could be ascribed to bulk MoO_3. The spectrum of the sample Mo(14)–P(4) (Fig. 2b), however, exhibited very intense bands associated with MoO_3 (compare with the spectrum of the bulk oxide (Fig. 2c)), in addition to a shoulder at 1005 cm^{-1} and a very weak band around 380 cm^{-1} due to the presence of bulk $Al_2(MoO_4)_3$ (20, 21). In the spectrum of the sample Mo(8)–P(4) (not shown), very weak bands appeared, and the high-fluorescence background of the spectrum made a clear assignment difficult. No

bands were observed for the sample Mo(14)–P(4)E.

A comparison of the XRD and LRS results confirms that both MoO_3 and $Al_2(MoO_4)_3$ crystalline phases grow as a result of phosphorus incorporation. The most reliable explanation of the formation of $Al_2(MoO_4)_3$ species for the present P-containing catalysts is the precipitation of the Al-molybdate just at the end of impregnation, when the molybdate solution is very concentrated; the Al^{3+} ions arise from partial solubilization of the alumina by phosphoric acid.

According to XRD, the lines corresponding to $Al_2(MoO_4)_3$ are much more intense than those due to MoO_3. This fact is probably associated with the better crystallinity of molybdate compared with that of MoO_3. On the other hand, compared with the intensity of the $Al_2(MoO_4)_3$ bands, the intensity of the bulk MoO_3 bands was much higher in
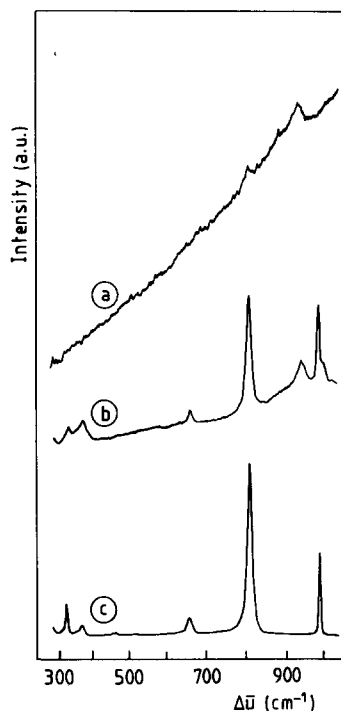

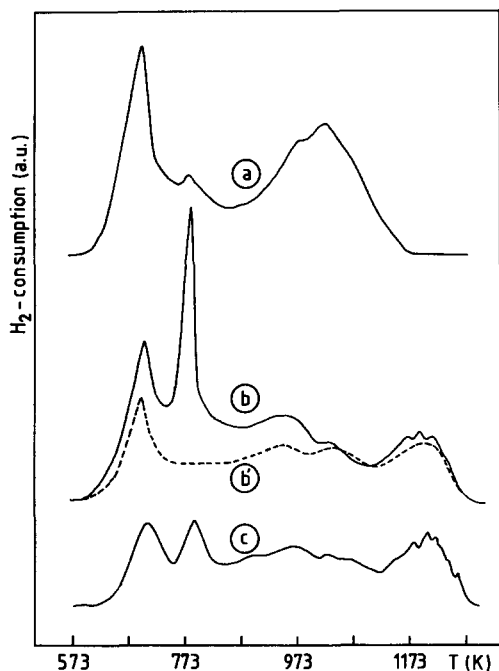FIG. 2. Raman spectra of (a) Mo(14)–P(0), (b) Mo(14)–P(4), and (c) bulk MoO_3.

FIG. 3. TPR profiles of (a) Mo(14)–P(0), (b) Mo(14)–P(4), (b') Mo(14)–P(4)E, and (c) Mo(8)–P(4).

LRS. These results suggest that MoO_3 is the most abundant surface phase, but its crystal size is almost at the detection limit (ca. 4.0 nm) of the conventional XRD technique.

The TPR profiles of the catalysts also showed marked differences (Fig. 3) which reflect the changes in Mo distribution indicated by the above XRD and LRS results. In agreement with previous findings (16), the comparison of TPR profiles of the P-containing catalysts (Figs. 3b and 3c) with that of the P-free counterpart (Fig. 3a) in the low temperature region shows the development of an intense peak with T_m (peak maximum) at about 785 K for the P-containing catalysts which was not found in the TPR profile of the Mo(14)–P(4)E sample (Fig. 3b'). The disappearance of this reduction peak in the ammonia-extracted sample is coincident with the lack of Mo-containing crystalline phases as shown by XRD and LRS.

An attempt to identify the origin of this TPR peak was made by recording the XRD

patterns of samples reduced in situ to different extents in a high-temperature diffraction camera. The XRD patterns corresponding to the reduction stages at 748 K (Fig. 4a) and 823 K (Fig. 4b) of the Mo(14)–P(4) catalyst are shown in Fig. 4. These temperatures correspond with the minimum H_2 consumption after the first and second TPR peaks. As can be seen, the presence of Mo-containing crystalline phases (MoO_3 and $Al_2(MoO_4)_3$) is still observed upon reduction at 748 K but not after reduction at 823 K, suggesting that the disappearance of such crystalline phases is associated with the second TPR peak (peak maximum, T_m = 785 K). Consistently, the low temperature peak (T_m ca. 700 K), assigned previously to the reduction of dispersed aggregates of molybdenum in multilayers (16, 22), is not related to reduction of the crystalline Mo species.

Further insight into the TPR at the 785 K peak was obtained through reduction of bulk MoO_3 and $Al_2(MoO_4)_3$ compounds under the same experimental conditions as the catalysts. It was found that the TPR profile of bulk MoO_3 exhibited a peak with T_m at ca. 890 K, corresponding to the reduction of Mo^{6+} to Mo^{4+}, and a second broader peak with T_m at ca. 1015 K with H_2 consumption consistent with the reduction of Mo^{4+} to Mo^0. The TPR profiles of $Al_2(MoO_4)_3$ showed a single broad reduction peak with T_m around 906 K and a H_2 consumption equivalent to the reduction of Mo^{6+} only up
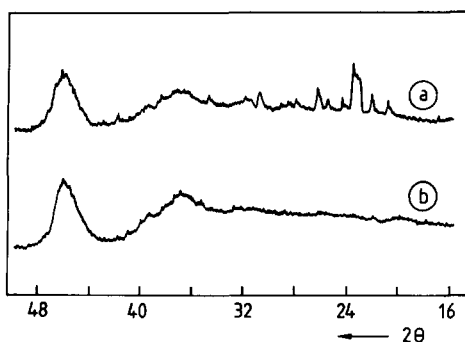

FIG. 4. X-ray diffraction patterns of Mo(14)–P(4) after TPR reduction at (a) 748 K and (b) 823 K.

to Mo^{5+} at temperatures lower than 1273 K. Thus, both MoO_3 and $Al_2(MoO_4)_3$ compounds have a first TPR peak with very similar T_m values, although at a temperature higher than that of the reduction peak of the crystalline species on the P–Al surface. Nevertheless, it may be noted that the shapes of the TPR profiles of bulk compounds are different from those obtained in supported systems (which generally shift to lower temperatures) due to the dispersion of the small crystals in a porous support and also, in this case, to the presence of previously reduced Mo species which could act as a catalyst for the subsequent reduction of MoO_3 and $Al_2(MoO_4)_3$. The fact that bulk MoO_3 was more reducible than $Al_2(MoO_4)_3$, as previously reported (23), suggests that the TPR peak at 785 K is due mainly to MoO_3 species.

CONCLUSIONS

From the above combined results it can be reasonably concluded that the observed TPR peak with T_m around 785 K for the P-containing Mo catalysts is associated with the reduction of crystalline MoO_3 and also some reduction of $Al_2(MoO_4)_3$. Note that formation of $Al_2(MoO_4)_3$ and MoO_3 is observed only at high Mo contents (>14 wt% MoO_3) and high calcination temperatures (>823 K) for P-free Mo catalysts (20, 21). In this case the formation of $Al_2(MoO_4)_3$ occurs by solid-state reaction of MoO_3 and Al_2O_3, while in the presence of phosphate it takes place during impregnation.

ACKNOWLEDGMENTS

REFERENCES

1. Haresnape, J. N., and Morris, J. E., British Patent 701.217, 1953.
2. Colgan, J. D., and Chomitz, N., U.S. Patent 3.287.280, 1966.
3. Morales, A. L., Galiasso, R. E., Ramirez de Agudelo, M. M., Salazar, J. A., and Carrasquel, A. R., U.S. Patent 4.520.128, 1985.
4. Fitz, C. W., and Rase, H. F., *Ind. Eng. Chem. Prod. Res. Dev.* **22**, 40 (1983).
5. Chadwick, D., Aitchison, D. W., Badilla-Ohlbaum, R., and Josefson, L., in "Preparation of Catalysts III" (G. Poncelet, P. Grange, and P. A. Jacobs, Eds.), p. 323. Elsevier, Amsterdam, 1983.
6. Stiegel, G. J., Tischer, R. E., Cillo, D. L., and Narain, N. K., *Ind. Eng. Chem. Prod. Res. Dev.* **24**, 206 (1985).
7. Gishti, K., Iannibello, A., Marengo, S., Morelli, G., and Tittarelli, P., *Appl. Catal.* **12**, 381 (1984).
8. Morales, A., and Ramirez de Agudelo, M. M., *Appl. Catal.* **23**, 23 (1986).
9. Bouwens, S. M. A. M., Vissers, J. P. R., de Beer, V. H. J., and Prins, R., *J. Catal.* **112**, 401 (1988).
10. Atanosova, P., Halachev, T., Uchytil, J., and Kraus, M., *Appl. Catal.* **38**, 235 (1988).
11. Ramirez de Agudelo, M. M., and Morales, A., in "Proceedings, 9th Int. Congress Catalysis, Calgary, 1988" (M. J. Phillips and M. Ternan, Eds.), Vol. I, p. 42. Chemical Institute of Canada, Ottawa, 1988.
12. Kemp, R. A., Ryan, R. C., and Smegal, J., in "Proceedings, 9th Int. Congress Catalysis, Calgary, 1988" (M. J. Phillips and M. Ternan, Eds.), Vol. I, p. 128. Chemical Institute of Canada, Ottawa, 1988.
13. Stanislaus, A., Absi-Halabi, M., and Al-Dolama, K., *Appl. Catal.* **39**, 239 (1988).
14. Morales, A., Ramirez de Agudelo, M. M., and Fernández, F., *Appl. Catal.* **41**, 261 (1988).
15. López Cordero, R., Gil Llambías, F. J., Palacios, J. M., Fierro, J. L. G., and López Agudo, A., *Appl. Catal.* **56**, 197 (1989).
16. López Cordero, R., Esquivel, N., Lázaro, J., Fierro, J. L. G., and López Agudo, A., *Appl. Catal.* **48**, 341 (1989).
17. Fierro, J. L. G., López Agudo, A., Esquivel, N., and López Cordero, R., *Appl. Catal.* **48**, 353 (1989).
18. Haller, G., McMillan, B., and Brinen, J., *J. Catal.* **97**, 243 (1986).
19. Jeziorowski, H., and Knözinger, H., *J. Phys. Chem.* **83**, 1166 (1979).
20. Zingg, D. S., Makovsky, L. E., Rischer, R. E., Brown, F. R., and Hercules, D. M., *J. Phys. Chem.* **84**, 2889 (1980).
21. Kasztelan, S., Payen, E., Toulhoat, H., Grimblot, J., and Bonnelle, J. P., *Polyhedron* **5**, 157 (1986).
22. López Cordero, R., Lázaro, J., Fierro, J. L. G., and López Agudo, A., in "Proceedings of the XI Iberoamerican Symposium on Catalysis, June 1988" (F. Cossio, O. Bermudez, G. del Angel, and R. Gómez, Eds.), p. 563. Intituto Mexicano del Petróleo, México, 1988.
23. Massoth, F. E., *J. Catal.* **30**, 204 (1973).